# Low Flagellar Motor Torque and High Swimming Efficiency of *Caulobacter crescentus* Swarmer Cells

Guanglai Li and Jay X. Tang
Physics Department, Brown University, Providence, Rhode Island

ABSTRACT We determined the torque of the flagellar motor of *Caulobacter crescentus* for different motor rotation rates by measuring the rotation rate and swimming speed of the cell body and found it to be remarkably different from that of other bacteria, such as *Escherichia coli* and *Vibrio alginolyticus*. The average stall torque of the *Caulobacter* flagellar motor was ~350 pN nm, much smaller than the values of the other bacteria measured. Furthermore, the torque of the motor remained constant in the range of rotation rates up to those of freely swimming cells. In contrast, the torque of a freely swimming cell for *V. alginolyticus* is typically ~20% of the stall torque. We derive from these results that the *C. crescentus* swarmer cells swim more efficiently than both *E. coli* and *V. alginolyticus*. Our findings suggest that *C. crescentus* is optimally adapted to low nutrient aquatic environments.

## INTRODUCTION

Flagellated bacteria swim by rotating long, thin, helical flagellar filaments, driven from the base by a reversible rotary motor. When protons (or sodium ions for the $Na^+$-driven motor of *V. alginolyticus*) flow through a flagellar motor, the motor converts the proton motive force into a torque that rotates the flagellar filament (1,2). The rotating filament generates a pushing or pulling force that propels the bacterium. The relationship between the torque and rotation rate of the motor has been measured for a few bacterial species (3,4). At low rotation rates, the motor works at a nearly constant torque $T_0$, called the stall torque, until a knee rate, $\omega_{\text{knee}}$. Above the knee rate, the torque decreases linearly to zero, at the zero torque rate $\omega_0$. The number of protons passing through the *Streptococcus* flagellar motor per revolution of rotation has been measured to be constant at rotation rates up to 65 Hz and thus the energy consumed by the motor per revolution is also constant (5). The constant number of protons per revolution has been assumed for the flagellar motor of *E. coli* in the full range of rotation rates (3). With this assumption, all the proton motive force is converted to torque in the constant torque region (3). Above the knee rate, the torque $T$ is smaller than $T_0$ and only $T\omega$, out of the total proton motive force $T_0\omega$, is converted to torque. The remaining portion of the energy, $(T_0 - T)\omega$, is dissipated in the motor (3). Bacterial flagellar motors of different species are similar in structure (6–8), and so the knowledge described above is likely applicable to most, if not all, bacterial flagellar motors.

When bacteria swim freely in water, the flagellar motor can rotate very fast. If the motor operates at a rotation rate above the knee rate, the efficiency of converting the proton motive force to torque is less than unity. For example, the motor of freely swimming *V. alginolyticus* operates at a torque ~20% of the stall torque (4), and thus the energy conversion efficiency is only 20%. The energy consumed by the flagellar motor, however, is usually negligible compared to its total energy cost during growth (9). Thus, in a rich environment where the supply of nutrients is sufficient, the low efficiency of the motor does not pose a problem for a bacterium. For a fast swimming bacterium in a low nutrient environment, however, the flagellum spends a significant percentage of the total available energy budget on movement, and so a high energy efficiency of swimming may be selected over the course of evolution (10,11).

*Caulobacter* is a bacterium that survives in very low nutrient environments (12,13). It has two morphologies in its life cycle—the swarmer cell and the stalked cell (14). The stalked cell can attach to a surface by its holdfast and its long stalk may help in the uptake of nutrients (15). The swarmer cell has a polar flagellum which it uses to swim to places with more nutrients. The swarmer cell is largely biochemically inert and so the majority of its energy consumption is spent on swimming (16). In this article, we study the torque of the flagellar motor of *Caulobacter* swarmer cells under various conditions. We show through this work that these cells swim both fast and efficiently, suggesting that they have optimally adapted to a low nutrient aquatic environment through the course of evolution.

## MATERIALS AND METHODS

### Strains

*Caulobacter crescentus* CB15 wild-type and a mutant-lacking pilus, ΔPilin (YB 375), were used in the experiments. They were grown in the PYE (0.2% peptone, 0.1% yeast extract, 0.6 mM $MgSO_4$, and 0.5 mM $CaCl_2$) medium (12) overnight at 30°C. One milliliter of the overnight culture was centrifuged and the pellet was resuspended in 10 ml of fresh PYE or M2G (20 mM total of sodium phosphate and potassium phosphate, 9.3 mM $NH_4Cl$, 0.5 mM $MgSO_4$, 0.5 mM $CaCl_2$, 0.01 mM $FeSO_4$, 0.008 mM EDTA, and

*Submitted January 3, 2006, and accepted for publication June 26, 2006.*

Address reprint requests to J. X. Tang, Tel.: 401-863-2292; E-mail: jay_tang@brown.edu.

© 2006 by the Biophysical Society

0006-3495/06/10/2726/09 $2.00

doi: 10.1529/biophysj.106.080697

0.2% glucose, pH = 7.06) medium (12). The cells were further grown for 5 h at 30°C to the midexponential phase. The culture was then centrifuged and resuspended again in various fresh media for motility measurements. The media were oxygenated in 9-cm plates with gentle shaking for >5 h before use.

## Media for motility measurements

We measured the rotation rate and swimming speed of the cell body of the swarmer cells in various media. The media PYE, M2G, M2 salts (M2G without glucose) (12), and deionized water were used to study the effects of different levels of nutrients. Dialyzed and lyophilized Ficoll 400 (Sigma-Aldrich, St. Louis, MO) of concentration up to 5% w/v in the M2 salts solution and glycerol of concentration up to 20% v/v in the M2 salts solution were used to investigate the motor behavior in viscous media. To study the influence of pH level, we adjusted the pH values of M2 salts from 5 to 9 by adding 1 M HCl or NaOH.

## Measurement of rotation rate and swimming speed of cell body

To make a slide sample for light microscopy observation, a 10-$\mu$l suspension of the cells was placed between a glass slide and a coverslip and sealed with vacuum grease. In the slide sample, the swarmer cells were either swimming freely in the medium or attached to the glass surface. They were observed in phase contrast under an inverted light microscope (Nikon TE2000, Tokyo, Japan) with an oil immersion objective lens (100× Plan Apo, Nikon). All the measurements were performed at 23°C. The rotation and swimming of the cell body were recorded by a fast camera (Fastcam PCI R2, Photron USA, San Diego, CA) at 500 frames per second with the pertinent software (Fastcam Viewer, Photron USA). The rotation rate and swimming speed of the cell body were obtained by analyzing the video frame by frame. The detection of body rotation was aided by the crescent shape of the cell body. The rotation rate of the tethered cell body was measured in the same way.

## Measurement of flagellar filament lengths

The swarmer cells were dried on the coverslip and imaged with a Nanoscope IIIa Dimension 3100 (Digital Instruments, Santa Barbara, CA) atomic force microscope (AFM) using the contact mode in air. The lengths of the flagellar filaments were measured from the AFM images.

## Calculation of torque and rotation rate

Using the fast camera, we measured the swimming speed $v_c$ and rotation rate $\omega_c$ of the cell body of a swimming cell simultaneously. We can calculate from these measurements the torque $T_m$ and the rotation rate $\omega_m$ of the flagellar motor, following the treatment of Magariyama and co-workers (17,18). We outline below the derivation from the published work, which yields all the formulas applied in this work. This treatment is reliable and applicable to the typical parameters of the flagellated bacteria. It does, however, ignore the hydrodynamic coupling in the flow field caused by segments along the helical filament. A more rigorous analysis has been recently published to address this issue (19), but the corrections shown are smaller than the measurement errors and thus have been neglected in this work.

For simplicity, we treat all the torques and forces to be positive values. The equations of motion are

$$F_c - F_f = 0, \tag{1}$$

$$T_c - T_m = 0, \tag{2}$$

$$T_f - T_m = 0. \tag{3}$$

In these equations, $F_c = \alpha_c v_c$ and $T_c = \beta_c \omega_c$ are the drag force and torque acting on the cell body, where $\alpha_c$ and $\beta_c$ are the translational and rotational drag coefficients of the cell body. $F_f = \gamma_f \omega_f - \alpha_f v_c$ and $T_f = \beta_f \omega_f - \gamma_f v_c$ are the drag force and torque acting on the flagellar filament, where $\alpha_f$ and $\beta_f$ are the translational and rotational drag coefficients of the flagellar filament along the helical axis. The coefficient $\gamma_f$ is defined as the ratio of the propulsive force of the rotating flagellar filament to its rotation rate, i.e., $F = \gamma_f \omega_f$.

From the equations above, one can calculate the motor torque from either the swimming speed or rotation rate of the cell body

$$T_m = \frac{\alpha_c \beta_f + \alpha_f \beta_f - \gamma_f^2}{\gamma_f} v_c, \tag{4}$$

$$T_m = \beta_c \omega_c. \tag{5}$$

The rotation rate of the flagellar motor is the sum of the rotation rates of the cell body $\omega_c$ and the flagellar filament $\omega_f$. It is calculated by either

$$\omega_m = \omega_c + \omega_f = \omega_c + \frac{\alpha_c + \alpha_f}{\gamma_f} v_c \tag{6}$$

or

$$\omega_m = \left[\frac{(\alpha_c + \alpha_f)(\beta_c + \beta_f) - \gamma_f^2}{\beta_c \gamma_f}\right] v_c. \tag{7}$$

Assuming that the cell shape is a prolate ellipsoid of width $2a$ and length $2b$ in a liquid of viscosity $\eta$,

$$\alpha_c = 6\pi\eta a\left[1 - \frac{1}{5}\left(1 - \frac{b}{a}\right)\right], \tag{8}$$

$$\beta_c = 8\pi\eta a^3\left[1 - \frac{3}{5}\left(1 - \frac{b}{a}\right)\right]. \tag{9}$$

The helical flagellar filament is defined by its pitch $p$, helical radius $r$, the length of the filament $L$, and the cross-sectional diameter of the filament $2d$. The notation here is kept consistent with the literature (17), which has also provided the expressions of the coefficients as listed below:

$$\alpha_f = \frac{2\pi\eta L}{[\ln(2p/d) - 1/2](4\pi^2 r^2 + p^2)}(8\pi^2 r^2 + p^2), \tag{10}$$

$$\beta_f = \frac{2\pi\eta L}{[\ln(2p/d) - 1/2](4\pi^2 r^2 + p^2)}(4\pi^2 r^2 + 2p^2) r^2, \tag{11}$$

$$\gamma_f = \frac{2\pi\eta L}{[\ln(2p/d) - 1/2](4\pi^2 r^2 + p^2)} 2\pi r^2 p. \tag{12}$$

The rotation rate of the flagellar motor of a tethered cell is the rotation rate of the cell body since the flagellar filament is tethered to a surface and cannot rotate. The torque of the flagellar motor for a tethered cell is therefore calculated directly from Eq. 5.

# RESULTS

## Torque and rotation rate of the flagellar motor of freely swimming *Caulobacter* cells in different media

The average flagellar filament length of 34 filaments measured by AFM was 6.0 $\mu$m. The other parameters of a *Caulobacter* flagellar filament are quoted from the literature as $d = 0.007$ $\mu$m, $p = 1.08$ $\mu$m, and $r = 0.13$ $\mu$m

(20). Calculated from Eqs. 10–12, the drag coefficients of the filament are $\alpha_f = 9.8 \times 10^{-9}$ N m s$^{-1}$, $\beta_f = 2.0 \times 10^{-22}$ N m s rad$^{-1}$, and $\gamma_f = 4.5 \times 10^{-16}$ N s rad$^{-1}$.

Fig. 1 shows a time series of the swimming and rotation of a *Caulobacter* swarmer cell taken at 500 frames per second using the fast camera. Since the *Caulobacter* swarmer cell is slightly crescent-shaped, it is easy to visually detect the rotation of the cell body using the fast camera. The swimming speed and rotation rate of the cell body were measured from the recorded movie. We can then use either Eq. 4 or Eq. 5 to calculate the torque. The rotational drag coefficient of the cell body $\beta_c$, however, is very sensitive to the cell half-width $a$, which is hard to measure precisely. In addition, the crescent-shaped cell body is approximated to be a spheroid, thus a nominal half-width $a$ must be used rather than the actual half-width of the cell. Since the two equations must give the same torque, we can use them to determine $a$. Knowing that the cell half-length $b$ is ~0.8 $\mu$m, we found that setting $a$ to 0.25 $\mu$m yields the most consistent results for the torque from the two independent calculations. The calibration done with Eqs. 6 and 7 gives a similar value of $a$. Accordingly, the translational and rotational drag coefficients, $\alpha_c$ and $\beta_c$, of such a cell body can be calculated with Eqs. 8 and 9, yielding $\alpha_c = 6.8 \times 10^{-9}$ N s m$^{-1}$ and $\beta_c = 9.1 \times 10^{-22}$ N m s rad$^{-1}$. After the most acceptable value of $a$ is determined, we only use Eqs. 4 and 7, unless otherwise specified, to calculate the torque and rotation rate of the flagellar motor of freely swimming cells. This procedure avoids the much larger effect of the cell-width on rotational drag than on translational drag. The reasonable cell half-width is from 0.2 to 0.3 $\mu$m and the flagellar filament length we measured for 34 filaments by AFM is from 5.3 to 6.6 $\mu$m. With the proper treatment as described above, the errors in the calculated torque and rotation rate caused by the errors in the cell half-width and filament length are estimated to be <5%.

We measured the swimming speed before and after a cell reversed its swimming direction and found that the cell swims at the same speed in the opposite directions (data not shown). The flagellar motor switches its rotation direction between clockwise (CW) and counterclockwise (CCW) when the cell reverses its swimming direction. So there is no observable difference in the torque and rotation rate between CW and CCW rotations. Hereafter, we do not distinguish between the CW and CCW rotations of the flagellar motor.

Table 1 summarizes the swimming speed, torque, and rotation rate of the *Caulobacter* flagellar motor for freely swimming cells in various media. The motors of the two strains tested have similar values of torque in the same medium. The maximum torque is ~440 pN nm at a motor rotation rate of ~400 revolutions per second (rps) in M2G medium. The torque drops to <300 pN nm in deionized water, where the nutrient level is extremely low. Swarmer cells can swim in a pH range of 5–9. Fig. 2 shows the dependence of torque on the pH value for freely swimming cells of the ΔPilin strain in M2 salts. The torque increases from pH 5 to pH 7 and the dependence is weak between pH values of 7 and 9. These results indicate that the torque and rotation rate of the flagellar motor do not vary dramatically with regard to the nutrient or pH level of the environment.

## Comparison of flagellar motor torque between freely swimming and tethered *Caulobacter* cells

The swarmer cell of the CB15 wild-type has pili. When the cell is attached to the glass surface, the pili are also capable of sticking to the surface. The rotation of the tethered cell body therefore is different and more complicated than that of freely swimming cells. To compare the motor torque of tethered cells with that of freely swimming cells, we use the strain ΔPilin. The swarmer cell of this strain has no pilus and occasionally attaches to the glass surface by the flagellar filament. By focusing on the cell body and the dirt on the glass surface separately under the microscope, we found that the cell body typically stays a few micrometers from the surface. With this separation, the interaction between the cell body and the surface is negligible. The cell body also rotates along its long axis, much like that of a freely swimming cell. The torque of the tethered cell can be calculated directly using Eq. 5 and the motor rotation rate is simply that of the cell body.

We measured the rotation rate of the cell body for both the tethered and swimming cells of strain ΔPilin in M2 salts in the same slide samples, to avoid the variation caused by separate preparations. In each slide sample, some cells were tethered to the surface and some were swimming. The measured torque of tethered cells for a particular preparation was 323 ± 51 pN nm for a motor rotation rate of 47 ± 7.1 rps averaged over 20 cells (Fig. 3). The measured torque of swimming cells was 342 ± 52 pN nm for a motor rotation

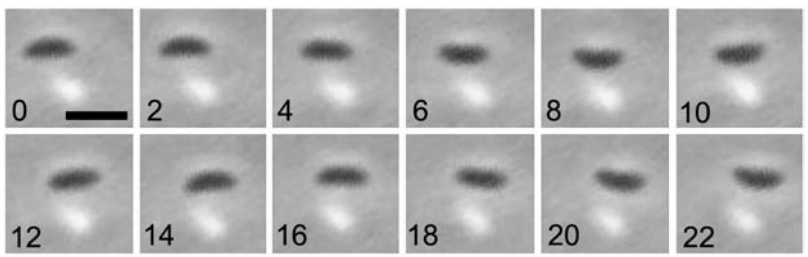


FIGURE 1 Time series of the swimming and rotation of a *Caulobacter* swarmer cell in M2 salts taken at 500 frames per second. A nonswimming cell out of the focal plane appears as a white spot, serving as a reference position. The swimming cell in the focal plane appears dark, and is noted to move from left to right. Numbers indicate time in milliseconds. The scale bar represents 2 $\mu$m. Images of the slight crescent shape indicate the rotation of the cell body. Each revolution of the cell body takes ~12 ms.

**TABLE 1 Average torque and rotation rates of flagellar motors of freely swimming cells averaged over 20 cells in various media**

| Strain | Medium | Swimming speed ($\mu$m/s) | Motor torque (pN nm) | Motor rotation rate (rps) |
|---|---|---|---|---|
| WT | PYE | 53.6 ± 6.8 | 392 ± 50 | 355 ± 45 |
| | M2G | 56.4 ± 5.4 | 414 ± 40 | 375 ± 36 |
| | M2 salts | 53.9 ± 5.6 | 395 ± 41 | 358 ± 37 |
| | water | 41.3 ± 7.3 | 303 ± 53 | 275 ± 48 |
| ΔPilin | PYE | 54.7 ± 6.6 | 402 ± 48 | 363 ± 43 |
| | M2G | 59.7 ± 7.3 | 437 ± 54 | 397 ± 48 |
| | M2 salts | 51.9 ± 5.4 | 380 ± 39 | 343 ± 35 |
| | water | 38.8 ± 6.9 | 286 ± 51 | 258 ± 46 |

WT, wild-type. Errors are the standard deviation.

rate of 310 ± 47 rps. The ratio of the motor torque of tethered cells to those swimming freely is 0.96. These results show that the torque of the motor is practically the same when rotating at a high speed of 310 rps as when rotating at a low speed of 47 rps, suggesting that the motor works at a constant torque up to or beyond the rotation rate of the motor of freely swimming cells.

Note here that the torque and rotation rate of the swimming cells quoted above are slightly lower than what are listed in Table 1 for the same ΔPilin strain in M2 salts (380 ± 39 pN nm and 343 ± 35 rps, respectively). The measurements yielding the results in Table 1 were performed with a different preparation of cells. This 10% variation is comparable to the range of errors among cells within a preparation as well.

## Torque-rotation rate relationship of *Caulobacter* flagellar motor

To confirm that the motor works at a constant torque up to the rotation rate of the motors of freely swimming cells, we measured the torque and rotation rate of the motors of swimming cells in the medium of M2 salts with elevated values of viscosity. We first tried to vary the viscosity by adding Ficoll 400 into the medium. In our observations, however, when the Ficoll 400 concentration was >5%, many swarmer cells stop swimming and some of them stuck together. We recorded the swimming of *Caulobacter* swarmer cells in 2% and 5% Ficoll solutions. The bulk viscosity of Ficoll 400 solution at 22.7°C (3) was used for the calculation. The torque and rotation rate of the motor calculated from the swimming speed using Eqs. 4 and 7 and from the rotation rate of the cell body using Eqs. 5 and 6 differ significantly from each other (Fig. 3 *a*). There are two possible causes of the difference. The first cause is the interaction between Ficoll 400 and the cells, which is obvious based on our observation when the Ficoll concentration is >5%. It is reasonable to speculate that such an interaction also exists to a certain extent at a lower concentration. The second likely cause is the polymer nature of Ficoll 400. Ficoll 400 is a highly branched polymer and the hydrodynamics of swimming bacteria in Ficoll solution is quite different from that in linear polymer solution (21). Ficoll is unlikely to form

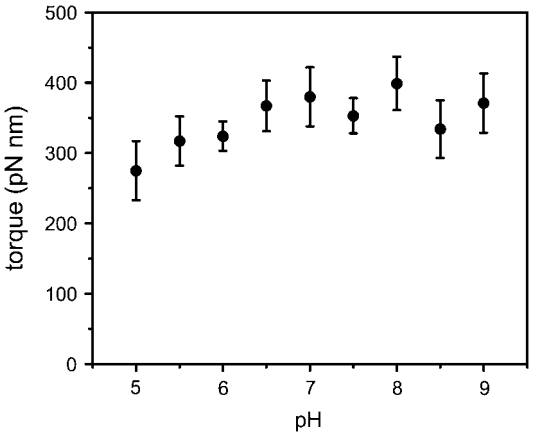


FIGURE 2 Torque of the flagellar motor of freely swimming cells in M2 salts at various pH values. Error bars indicate the standard deviation.

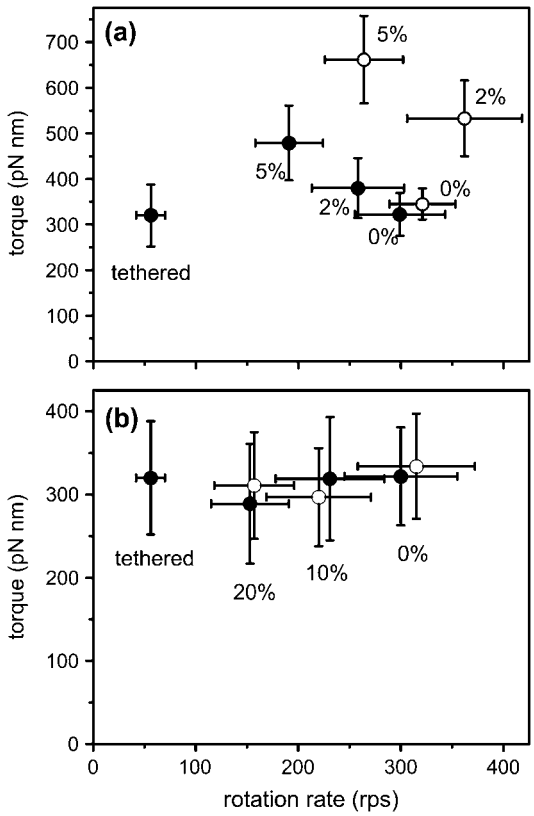


FIGURE 3 Torque-rotation rate relationship of the *Caulobacter* flagellar motor in M2 salts, with Ficoll (*a*) or glycerol (*b*). Concentration is w/v % for Ficoll and v/v % for glycerol. The open symbols are calculated from the swimming speed using Eqs. 4 and 7 and the solid symbols are calculated from the rotation rate of cell body using Eqs. 5 and 6, respectively. The data point for tethered cells is taken from panel *a* for close comparison. Error bars are the standard deviation.

networks in solution as the long linear polymer molecules do (22). Down at the sizes of the cell body in the submicrometer scale and of the flagellar filament diameter in the nanometer scale, however, the hydrodynamics of the cell with Ficoll is not clearly defined. It is possible that the local viscosities for the motions of a microscopic body in the directions tangential and normal to the surface are different from the bulk viscosity of the Ficoll solution and from each other (17).

To avoid this difficulty, we varied the viscosity with glycerol, which consists of small molecules only. Bacteria, however, can metabolize glycerol, and therefore the nutrient environment and intracellular pH value may be altered. Such an altered environment may in turn affect the motor behavior. As we measured, however, the torque does not change dramatically in the wide range of pH values and nutrient environments (Table 1 and Fig. 2). Therefore, the metabolization of glycerol is not expected to change the motor torque seriously. Fig. 3 *b* shows the torque of the motor at different rotation rates in glycerol solutions. The torques calculated from the swimming speed and that from the rotation rate of the cell body agree with each other well. This figure confirms that the motor works at the stall torque up to the rotation rate of the motor for freely swimming cells. As we know, the measurement varies from preparation to preparation. Later in the discussion, we shall refer to the stall torque as 350 pN nm and the motor rotation rate as 330 rps for freely swimming cells in M2 salts.

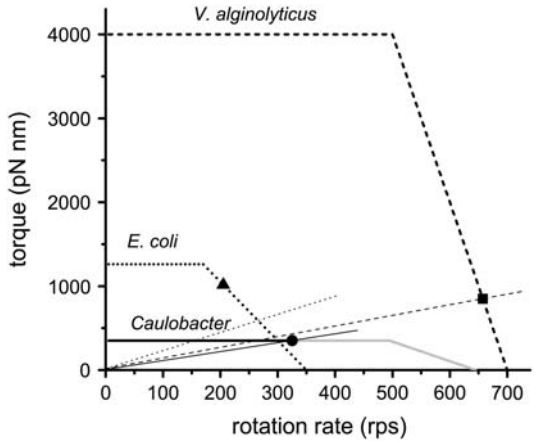


FIGURE 4 Comparison of the torque-rotation rate relationship of three bacteria species, *E. coli* (*dotted line*) (3,23), *V. alginolyticus* (*dashed line*) (4), and *Caulobacter* (*solid line*; this work). Shaded lines for *Caulobacter* cover the range of high rotation rates, in which the torque values are not measured. Symbols indicate the measured torque and rotation rates of the motor for freely swimming cells of *E. coli* (*triangle*), *V. alginolyticus* (*square*), and *Caulobacter* (*circle*). The thin lines are the calculated load lines for a single flagellar filament of *E. coli* (*dotted*; assumed in isolation), *V. alginolyticus* (*dashed*), and *Caulobacter* (*solid*). The motor rotation rate of freely swimming *E. coli* is estimated based on the measured rotation rate of the flagellar bundle (24).

## DISCUSSION

The torque-rotation rate relationships of the flagellar motors of *E. coli* and *V. alginolitycus* have been previously measured. The torque is nearly constant at low rotation rates and decreases linearly above a knee rotation rate. The stall torque of the flagellar motor is ~1260 pN nm for *E. coli* in the motility medium (23) and ~4000 pN nm for *V. alginolitycus* in a medium containing 50 mM NaCl (4). The motor rotation rate of freely swimming cells of *V. alginolitycus* is higher than the knee rate and the torque is much lower than the stall torque (4). An *E. coli* cell is propelled by a bundle of flagellar filaments. The rotation rate of a flagellar motor of a swimming *E. coli* cell is ~200 rps (24), which is slightly above, but close to, the knee rate. For a single flagellum of *E. coli*, however, the load line of the flagellar motor is calculated to be along the thin dotted line in Fig. 4. It intercepts with the experimentally measured torque-rotation rate curve much below the plateau region, suggesting that the calculated motor torque is much smaller than the stall torque. To resolve this discrepancy from actual experimental result (24), the rotational drag of a flagellar filament in a bundle would have to be more than twice the value when it rotates out of a bundle. The large increase in the rotational drag is probably due to the hydrodynamic and mechanical interactions among the filaments in the flagellar bundle, but a quantitative treatment is currently lacking. Another study based on measurements several years earlier shows that the stall torque is ~4600 pN nm (25). If this value is right, the rotational drag of a flagellar filament in a bundle would have to be seven times larger than when it rotates out of a bundle. We will use the lower stall torque of the flagellar motor of *E. coli*, 1260 pN nm, in the ensuing discussion.

The torque-rotation rate plot of a *Caulobacter* flagellar motor has two remarkable features in comparison with that of the other species measured, as depicted in Fig. 4: 1), the average stall torque of 350 pN nm is much smaller than *E. coli* and *V. alginolitycus*; and 2), the rotation rate of the flagellar motor of freely swimming cells is lower than the knee rotation rate. Due to the similarities in structure, however, the *Caulobacter* flagellar motor is expected to share the main features observed for other bacteria. The flagellar motor of *streptococcus* converts the proton motive force into torque, with the number of protons translocated through the motor constant per revolution (5). Hereafter in the discussion, we assume a constant number of protons (or sodium ions) per revolution of the flagellar motor of the three bacterial species in the full range of rotation rates. The motor is nearly 100% efficient in its energy conversion in the range of constant torque. Above the knee rotation rate, the conversion efficiency drops with the torque (3). Based on the measured torque-rotation curve (Fig. 4), the energy conversion efficiency of the motor of a swimming cell is only 20% for *V. alginolyticus*, but in principle 100% for *Caulobacter* swarmer cells. The energy conversion efficiency of *E. coli* is also very high, at ~80% or more. A much larger torque,

however, is required for *E. coli* to generate a comparable swimming speed to *Caulobacter* swarmer cells.

In the following paragraphs we discuss the implications of the small stall torque on the biological functions of *Caulobacter*. To facilitate our discussion, we introduce a new parameter called the swimming efficiency of a flagellated bacterium, which is defined as the ratio of the swimming speed to the energy consumption rate of the flagellar motors. It is also the ratio of the swimming distance to the energy consumed, much like in the miles per gallon of an automobile. The swimming efficiency reflects how efficiently a flagellated bacterium swims with regard to its energy consumption. It is different from the motor efficiency of energy conversion (3), which is the percentage of consumed energy converted to work by the flagellar motor. It is also different from the propulsion efficiency (9,18), which describes the ratio of energy used to overcome the drag during swimming.

The swimming speed depends on the rotation rate of flagellar motor as

$$v_c = f\omega_m, \tag{13}$$

where

$$f = \frac{\beta_c \gamma_f}{(\alpha_c + \alpha_f)(\beta_c + \beta_f) - \gamma_f^2} \tag{14}$$

is a geometric parameter. Replacing these drag coefficients in Eq. 14 with Eqs. 8–12, we find that the geometric parameter is independent of the viscosity and determined only by the size and shape of the cell body and the flagellar filament. The total energy consumption per unit time by the motor is $T_0\omega_m$ and therefore the swimming efficiency is

$$\varepsilon = f/T_0. \tag{15}$$

The swimming efficiency is clearly defined by two factors: it is proportional to the geometric parameter $f$ and inversely proportional to the stall torque $T_0$ of the flagellar motor. To our knowledge, there is no previous study of the swimming behavior of *Caulobacter* in a viscous medium. Nevertheless, our analysis predicts that the swimming efficiency does not depend on the viscosity of the medium.

Now let us compare the swimming efficiency of the three bacteria, *Caulobacter*, *E. coli*, and *V. alginolitycus*. All relevant numbers are summarized in Table 2. Calculated from Eq. 15, the swimming efficiency is $5.1 \times 10^9$ m/J for *V. alginolyticus*, and $6.7 \times 10^{10}$ m/J for *Caulobacter*. An *E. coli* cell has several flagella, with the average number approximated to be 4. When the cell swims, the four flagellar filaments form a bundle with a diameter assumed to be ~30 nm. The swimming efficiency for *E. coli* is calculated as the geometric factor for the bundle divided by the sum of the stall torque of all motors ($4 \times 1260$ pN nm, for example, assuming four motors), which yields a low value of $7.3 \times 10^9$ m/J. In conclusion, *Caulobacter* swims an order-of-magnitude more efficiently than either of the other bacteria (Fig. 5 *a*).

The swimming efficiency is not very sensitive to flagellar filament length within a reasonable range (Fig. 5 *a*). *Caulobacter* flagellar filament length varies from cell to cell in the range of 5.3 to 6.6 $\mu$m as measured by AFM. The flagellar filament length of *V. alginolitycus* is reported as $5.02 \pm 1.15$ $\mu$m (18). The distribution of the flagellar filament lengths of *E. coli* has not been measured, but it is a safe estimate that the lengths fall in the range from 5 to 10 $\mu$m. Within the ranges specified, the geometric parameter $f$ of *Caulobacter* is comparable to that of *V. alginolitycus*. *E. coli* swims with a bundle of flagellar filaments, which gives rise to a slightly larger value of $f$ (Fig. 5 *b*). By

**TABLE 2 Parameters and calculated values for the three bacterial species**

| | *C. crescentus* | *E. coli* | *V. alginolyticus* |
|---|---|---|---|
| $L$, Length of flagellar filament ($\mu$m) | 6.0 | 7.3, (29)* | 5.02, (17) |
| $2d$, Diameter of flagellar filament ($\mu$m) | 0.014, (20) | 0.013, (30) | 0.032, (17) |
| $p$, Pitch of flagellar helix ($\mu$m) | 1.08, (20) | 2.5, (29) | 1.58, (17) |
| $r$, Radius of flagellar helix ($\mu$m) | 0.14, (20) | 0.19, (29) | 0.14, (17) |
| $2a$, Cell width ($\mu$m) | 0.5 | 1, (29)* | 0.80, (17) |
| $2b$, Cell length ($\mu$m) | 1.6 | 2, (29)* | 1.92, (17) |
| $T_0$, Stall torque (pN nm) | 350 | 1260, (23) | 4000, (17) |
| $\omega_0$, Rotation rate at zero torque (rps) | unknown | 350, (3) | 700, (4) |
| $\omega_{knee}$, Knee rotation rate (rps) | unknown | 170, (3) | 500, (4) |
| $\omega_{swim}$, Motor rate of swimming cells (rps) | 330 | ~206, (24)† | 650, (4) |
| $T_{swim}$, Motor torque of swimming cells (pN nm) | 350 | ~1000, (3,23,24) | 800, (4) |
| Energy conversion efficiency when swimming | ~100% | ~80% | 20% |
| Geometric parameter $f$ ($\mu$m/round) | 0.15 | 0.23 | 0.13 |
| $\varepsilon$, Swimming efficiency (m/J) | $6.7 \times 10^{10}$ | $7.3 \times 10^9$ | $5.1 \times 10^9$ |

The numbers in the parentheses are those of the listed references. The values without reference are obtained in this study. The swimming efficiency is calculated by assuming the cell swims along its long axis, driven by a single polar flagellum for *Caulobacter* and *V. alginolyticus*, and by a bundle of four filaments for *E. coli*.

*Estimated from the fluorescence image.

†Assuming the cell body rotates at 7% of the bundle.

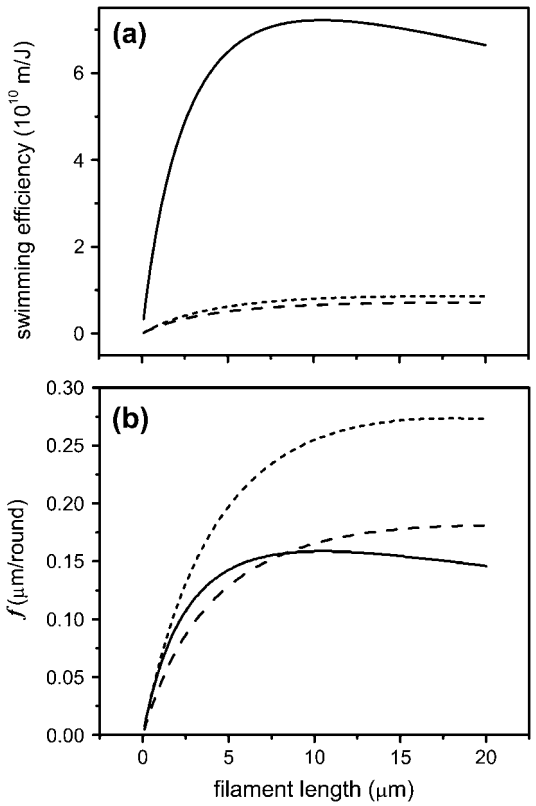


FIGURE 5 The swimming efficiency (*a*) and the geometric parameter $f$ (*b*) of *Caulobacter* (*solid*), *V. alginolitycus* (*long dash*), and *E. coli* (*short dash*).

comparing the plots in Fig. 5, *a* and *b*, with Eq. 15 in mind, it is clear that the higher swimming efficiency of *Caulobacter* is primarily due to its smaller stall torque. We conclude that the stall torque is the dominating factor in swimming efficiency.

The smaller cell size of *Caulobacter* does not mean a higher swimming efficiency. The length of a *Caulobacter* swarmer cell is comparable to that of *E. coli* and *V. alginolyticus*. The width of the *Caulobacter* cell body is smaller, but by less than a factor of two. Assuming fixed size and geometry of the flagellar filament and the length of the cell body, we calculate the swimming efficiency of *Caulobacter* as a function of the half-width of the cell body (Fig. 6). The half-width of a *Caulobacter* swarmer cell is ~0.25 μm, at which the swimming efficiency is close to the maximum. The swimming efficiency does not drop dramatically with increasing half-width. For example, if the half-width of a *Caulobacter* cell increases from 0.25 μm to 0.5 μm, which is close to the size of *E. coli* and *V. alginolyticus*, the swimming efficiency as defined in this work would drop by only 5%, from $6.7 \times 10^{10}$ m/J to $6.4 \times 10^{10}$ m/J. The total translational drag of a cell is the sum of the drag of the cell body and the flagellar filament. When the width of the cell body increases, the total translational drag also increases, and the cell will swim slower. But in the mean time, the

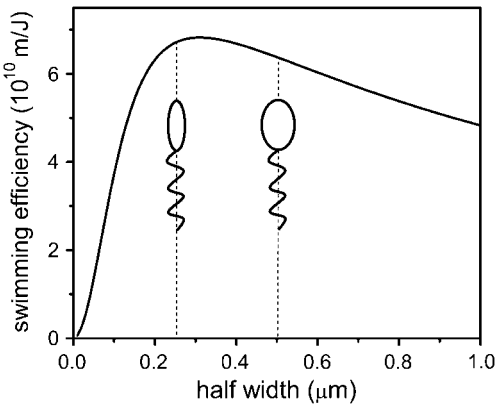


FIGURE 6 Dependence of *Caulobacter* swimming efficiency on the half-width of cell body. The insets are the schematic drawings of cells with half-widths of 0.25 and 0.5 μm, respectively.

flagellar motor will also rotate slower due to the increased width of the cell body. The energy consumption rate is proportional to the motor rotation rate. The swimming efficiency therefore, which is defined as the ratio of the swimming speed to the energy consumption rate, does not vary much when the cell width varies within the range of interest. Based on the analysis here, even if the *Caulobacter* cell had the same width as *E. coli* and *V. alginolyticus*, it would still swim more efficiently by an order of magnitude.

It is interesting to note that as the half-width of the cell body becomes unrealistically small, the swimming efficiency drops steeply (Fig. 6). This property is easy to understand, as well. When the width of the cell body is very small, its further decrease is expected to cause negligible reduction in translational drag, so the swimming speed does not increase noticeably. The decrease of the width of the cell body, however, leads to a dramatic decrease in rotational drag. This leads to an inversely proportional increase in the rotation rate of the cell body, and hence also the energy consumption rate of the motor. The swimming efficiency therefore drops steeply as the cell width approaches the lower limit.

From Eq. 15, the knee rotation rate, $\omega_{\text{knee}}$, and zero torque rotation rate, $\omega_0$, on the torque-rotation rate curve of the motor at a given stall torque, do not affect the swimming efficiency. They will, however, affect the swimming speed. The swimming speed depends on the torque as

$$v_c = T_m \gamma_f / [\beta_f(\alpha_c + \alpha_f) - \gamma_f^2]. \quad (16)$$

The torque is a function of the rotation rate of the motor as

$$T_m = T_0, \quad \text{when} \quad \omega_m < \omega_{\text{knee}} \quad (17)$$

and

$$T_m = T_0\left(1 - \frac{\omega_m - \omega_{\text{knee}}}{\omega_0 - \omega_{\text{knee}}}\right), \quad \text{when } \omega_0 \geq \omega_m \geq \omega_{\text{knee}}. \quad (18)$$

We now calculate the swimming speed of the cell with different flagellar filament lengths, assuming three sets of

relevant values of $\omega_{knee}$ and $\omega_0$ for the flagellar motor of *Caulobacter*. The knee rotation rate $\omega_{knee}$ was chosen to be smaller, equal, and larger than the rotation rate of the motor of a freely swimming cell, and the zero torque rate $\omega_0$ is assumed to be 50% larger than the knee rate. The calculated swimming speeds and swimming efficiency are shown in Fig. 7. The swimming efficiency as a function of the flagellar filament length is the same for all three cases. In the practically relevant range of filament lengths, the higher the knee rotation rate, the faster the swimming speed.

For *Caulobacter* swarmer cells to survive in a low nutrient environment, the flagellum needs to work efficiently. From Fig. 7, a flagellum achieves the best combination of swimming efficiency and swimming speed when the knee rotation rate is >350 rps, the measured motor rotation rate of free swimming cells. In our measurement, the *Caulobacter* swarmer cell indeed operates at a rate lower than the knee and therefore swims most efficiently.

There are many possible mechanisms for the *Caulobacter* flagellar motor to generate a very low stall torque. For example, the proton motive force might be very small, there might be fewer torque generating units, or the motor efficiency for torque generation might be low. *Caulobacter* is a gram-negative bacterium of motor structure similar to that of *E. coli*. It is reasonable to expect that its proton motive force is comparable to that of *E. coli* and other gram-negative bacteria, which is ~100–200 mV (26). There are ~38 protons translocated through each force-generating unit of the flagellar motor of *E. coli* per revolution of the motor rotation (23). The stall torque of *Caulobacter* is much smaller than the stall torque of *E. coli*. If we assume that *Caulobacter* has the same number of torque-generating units and the same motor efficiency for torque generation as *E. coli*, only ~12 protons would flow through each torque-generation unit per revolution (27). The stepwise rotation of the flagellar motor has been observed directly under reduced sodium motive forces (28). We speculate based on this work that the *Caulobacter* flagellar motor might be a good candidate for the detection of stepwise rotation driven by the translocation of single protons. This hypothesis is testable. Future experiments may help elucidate the molecular mechanism of the torque generation.

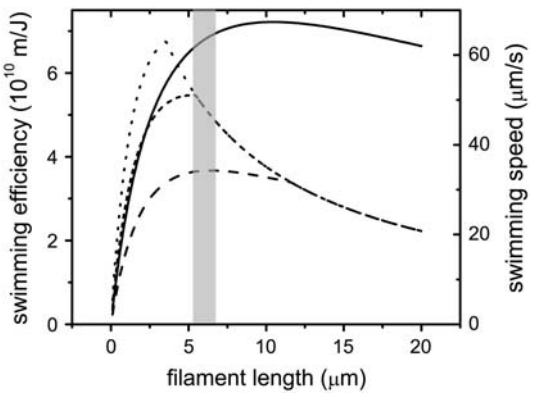


FIGURE 7 The swimming efficiency (*solid line*) and the swimming speed of *Caulobacter* cells as functions of flagellar filament length. The knee rotation rate of the flagellar motor is assumed to be 200 rps (*long-dashed line*), 350 rps (*short-dashed line*), and 500 rps (*dotted line*). The zero torque rotation rate is assumed to be 1.5 times that of the knee rotation rate. The lengths of most *Caulobacter* flagellar filaments fall in the shaded range.

In summary, we measured the torque and rotation rate of the flagellar motor of *Caulobacter* in various conditions. Remarkably, the average stall torque is ~350 pN nm, which is much smaller than the stall torque of *E. coli* or *V. alginolitycus*. The motor works at a constant torque up to its rotation rate in freely swimming *Caulobacter* cells at ~330 rps, whereas for *V. alginolitycus*, the torque of the motors in freely swimming cells is much smaller than the stall torque. These two features provide evidence for the adaptation of *Caulobacter* to low nutrient environments. *Caulobacter* swims very efficiently due to its small stall torque and in the meanwhile, maintains a high swimming speed because the motor operates at below the knee rotation rate while swimming.

We thank Professor Yves Brun at Indiana University for providing the *Caulobacter* strains and additional consultation. We also acknowledge helpful discussions with Drs. Howard Berg, Thomas Powers, Linda Turner-Stern, and Charles Wolgemuth.

This work was supported by National Science Foundation grant No. DMR 0405156, National Institutes of Health grant No. R01 HL 67286, and a Salomon Research Award, Brown University.

## REFERENCES

1. Manson, M. D., P. Tedesco, H. C. Berg, F. M. Harold, and C. van der Drift. 1977. A protonmotive force drives bacterial flagella. *Proc. Natl. Acad. Sci. USA.* 74:3060–3064.
2. Blair, D. F. 2003. Flagellar movement driven by proton translocation. *FEBS Lett.* 545:86–95.
3. Chen, X., and H. C. Berg. 2000. Torque-speed relationship of the flagellar rotary motor of *Escherichia coli*. *Biophys. J.* 78:1036–1041.
4. Sowa, Y., H. Hotta, M. Homma, and A. Ishijima. 2003. Torque-speed relationship of the $Na^+$-driven flagellar motor of *Vibrio alginolyticus*. *J. Mol. Biol.* 327:1043–1051.
5. Meister, M., G. Lowe, and H. C. Berg. 1987. The proton flux through the bacterial flagellar motor. *Cell.* 49:643–650.
6. Stallmeyer, M. J., K. M. Hahnenberger, G. E. Sosinsky, L. Shapiro, and D. J. DeRosier. 1989. Image reconstruction of the flagellar basal body of *Caulobacter crescentus*. *J. Mol. Biol.* 205:511–518.
7. Stallmeyer, M. J., S. Aizawa, R. M. Macnab, and D. J. DeRosier. 1989. Image reconstruction of the flagellar basal body of *Salmonella typhimurium*. *J. Mol. Biol.* 205:519–528.
8. Berg, H. C. 2003. The rotary motor of bacterial flagella. *Annu. Rev. Biochem.* 72:19–54.
9. Purcell, E. M. 1977. Life at low Reynolds-number. *Am. J. Phys.* 45: 3–10.
10. Mitchell, J. G. 1991. The influence of cell size on marine bacterial motility and energetics. *Microb. Ecol.* 22:227–238.
11. Mitchell, J. G. 2002. The energetics and scaling of search strategies in bacteria. *Amer. Naturalist.* 160:727–740.

12. Poindexter, J. S. 1981. The *Caulobacters*: ubiquitous unusual bacteria. *Microbiol. Rev.* 45:123–179.

13. Poindexter, J. S. 1964. Biological properties and classification of the *Caulobacter crescentus* group. *Bacteriol. Rev.* 28:231–295.

14. Li, G., C. S. Smith, Y. V. Brun, and J. X. Tang. 2005. The elastic properties of the *Caulobacter crescentus* adhesive holdfast are dependent on oligomers of *N*-acetylglucosamine. *J. Bacteriol.* 187: 257–265.

15. Ireland, M. M. E., J. A. Karty, E. M. Quardokus, J. P. Reilly, and Y. V. Brun. 2002. Proteomic analysis of the *Caulobacter crescentus* stalk indicates competence for nutrient uptake. *Mol. Microbiol.* 45: 1029–1041.

16. Koch, A. L. 2001. Oligotrophs versus copiotrophs. *Bioessays.* 23: 657–661.

17. Magariyama, Y., and S. Kudo. 2002. A mathematical explanation of an increase in bacterial swimming speed with viscosity in linear-polymer solutions. *Biophys. J.* 83:733–739.

18. Magariyama, Y., S. Sugiyama, K. Muramoto, I. Kawagishi, Y. Imae, and S. Kudo. 1995. Simultaneous measurement of bacterial flagellar rotation rate and swimming speed. *Biophys. J.* 69:2154–2162.

19. Kim, M., and T. R. Powers. 2005. Deformation of a helical filament by flow and electric or magnetic fields. *Phys. Rev. E.* 71:021914.

20. Koyasu, S., and Y. Shirakihara. 1984. *Caulobacter crescentus* flagellar filament has a right-handed helical form. *J. Mol. Biol.* 173: 125–130.

21. Nakamura, S., Y. Adachi, T. Goto, and Y. Magariyama. 2006. Improvement in motion efficiency of the spirochete *Brachyspira pilosicoli* in viscous environments. *Biophys. J.* 90:3019–3026.

22. Berg, H. C., and L. Turner. 1979. Movement of microorganisms in viscous environments. *Nature.* 278:349–351.

23. Reid, S. W., M. C. Leake, J. H. Chandler, C.-J. Lo, J. P. Armitage, and R. M. Berry. 2006. The maximum number of torque-generating units in the flagellar motor of *Escherichia coli* is at least 11. *Proc. Natl. Acad. Sci. USA.* 103:8066–8071.

24. Lowe, G., M. Meister, and H. C. Berg. 1987. Rapid rotation of flagellar bundles in swimming bacteria. *Nature.* 325:637–640.

25. Berry, R. M., and H. C. Berg. 1997. Absence of a barrier to backwards rotation of the bacterial flagellar motor demonstrated with optical tweezers. *Proc. Natl. Acad. Sci. USA.* 94:14433–14437.

26. Kashket, E. R. 1985. The proton motive force in bacteria: a critical assessment of methods. *Annu. Rev. Microbiol.* 39:219–242.

27. Ryu, W. S., R. M. Berry, and H. C. Berg. 2000. Torque-generating units of the flagellar motor of *Escherichia coli* have a high duty ratio. *Nature.* 403:444.

28. Sowa, Y., A. D. Rowe, M. C. Leake, T. Yakushi, M. Homma, A. Ishijima, and R. M. Berry. 2005. Direct observation of steps in rotation of the bacterial flagellar motor. *Nature.* 437:916–919.

29. Turner, L., W. S. Ryu, and H. C. Berg. 2000. Real-time imaging of fluorescent flagellar filaments. *J. Bacteriol.* 182:2793–2801.

30. Berg, H. C. 1975. Chemotaxis in bacteria. *Annu. Rev. Biophys. Bioeng.* 4:119–136.